ELSEVIER

Spectrochimica Acta Part B 52 (1997) 219–229

SPECTROCHIMICA ACTA PART B

Three-dimensional density profiles of argon metastable atoms in a direct current glow discharge: experimental study and comparison with calculations

A. Bogaerts[a,*], R.D. Guenard[b], B.W. Smith[b], J.D. Winefordner[b], W.W. Harrison[b], R. Gijbels[a]

[a]*Department of Chemistry, University of Antwerp (UIA), Universiteitsplein 1, B-2610 Wilrijk, Belgium*
[b]*Department of Chemistry, University of Florida, Gainesville, FL 32611, USA*

Received 8 May 1996; accepted 3 August 1996

Abstract

Three-dimensional density profiles of argon metastable atoms (Ar_m*) have been measured by laser-induced fluorescence in a direct current glow discharge with flat cathode, for a range of voltages, pressures and currents (i.e. 700–1200 V, 0.7–1.6 torr, 0.6–3.3 mA). The primary excitation line was taken to be the 794.818 nm line, whereas the 852.144 nm line was used as the fluorescence line. The profile is characterized by two distinct peaks, at 2–4 mm and about 12 mm from the cathode respectively. These peaks are explained as being caused by local Ar_m* production and loss processes, giving rise to local maxima which are not completely spread out by diffusion. The experimental data have been compared with the results of a mathematical model consisting of a balance equation with many production and loss terms. The theoretical profile also shows two peaks, but at somewhat different positions, and the first peak is much more intense. This suggests that the model is not yet able to describe the behavior of metastable atoms exactly, and that the glow discharge is hence more complex than often assumed. Nevertheless, comparison of the overall Ar_m* number density in the rest of the discharge volume indicates to us that a generally reasonable agreement has been reached between experiment and theory. © 1997 Elsevier Science B.V. All rights reserved.

Keywords: Argon metastable atoms; Direct current glow discharge; Laser-induced fluorescence; Diagnostic study; Three-dimensional profiles; Discharge modeling

1. Introduction

Glow discharges are used in analytical chemistry as atomization–excitation–ionization sources for mass spectrometry and optical spectrometric techniques [1,2]. For good analytical practice, a thorough understanding of the fundamental processes in the glow discharge is desirable. Both mathematical modeling and experimental plasma diagnostics are useful to achieve this.

The argon glow discharge is a complex plasma, consisting of a large number of species (electrons, argon atoms in the ground state, argon ions, metastable argon atoms, sputtered atoms and ions, etc.). The metastable argon atoms play an important role in the analytical glow discharge. Indeed, it is generally stated that ionization of the sputtered atoms occurs to a large extent by collisions with argon metastable atoms (Penning ionization). Some models have

* Corresponding author.

0584-8547/97/$17.00 Copyright © 1997 Elsevier Science B.V. All rights reserved
PII S0584-8547(96)01578-9

been described in the literature to calculate the metastable atom number densities of He [3–6], Ne [6] and Ar [6–10] in a glow discharge. The models are all based on a balance equation taking into account the different production and loss processes of the metastable atoms. Since a number of production and loss processes come into play, the models can be very complicated. Results of such models comprise the metastable atom number density profiles, mostly in one dimension, except in ref. [10] where three-dimensional number density distributions have been calculated.

Atomic absorption measurements of metastable atom densities in a glow discharge have also been reported in the literature, e.g. for He [3–5,11], Ne [12] and Ar [7,13–15]. Most of these results are presented for only one position in the plasma, except in refs. [3–5,14] where spatially resolved measurements were carried out yielding one-dimensional number density profiles. To our knowledge, three-dimensional density profiles of Ar metastables have not yet been measured. Conventional atomic absorption measurements with non-laser sources are, in principle, not well suited to perform such measurements, since only integrated values are obtained. To acquire three-dimensional number density profiles, laser-induced fluorescence has to be employed.

The absolute values of the number densities obtained by the measurements reported in the literature range from 10^{10}–10^{11} cm^{-3} (e.g. refs. [5,7,12,15]) over 10^{11}–10^{12} cm^{-3} (e.g. refs. [3,4,13]) to 10^{12}–10^{13} cm^{-3} (e.g. refs. [11,14]), depending on the discharge conditions and the cell geometry. It is therefore difficult to make direct comparisons between the different results.

In order to check the results of the model of ref. [10] (i.e. to test whether the different production and loss processes taken into account yield a realistic picture of the glow discharge), experimental measurements are required for the same cell geometry and the same discharge conditions as are used in the model. In the present paper, laser-induced fluorescence is used to measure three-dimensional absolute number density profiles for the argon metastable atoms. The experimental data will be compared with the results of the three-dimensional model [10] calculated for the same geometry.

2. Theoretical background

Laser-induced fluorescence measurements yield a three-dimensional fluorescence intensity profile. From the fluorescence intensity, the number density of the argon metastable atoms can be calculated. Fig. 1 shows a part of the energy level scheme of Ar, relevant for these experiments. The Paschen notation is used to identify the energy levels. The argon atom ground state lies at 0 cm^{-1} and is not indicated. The $1s_3$ and $1s_5$ levels are both metastable (i.e. long-lived) levels; the $1s_2$ and $1s_4$ levels are levels which can decay to the ground state by emission of radiation. The different excitation lines from the 1s levels to the 2p levels are also indicated, together with their oscillator strengths [16]. The numbers between brackets at the right of the scheme represent the level

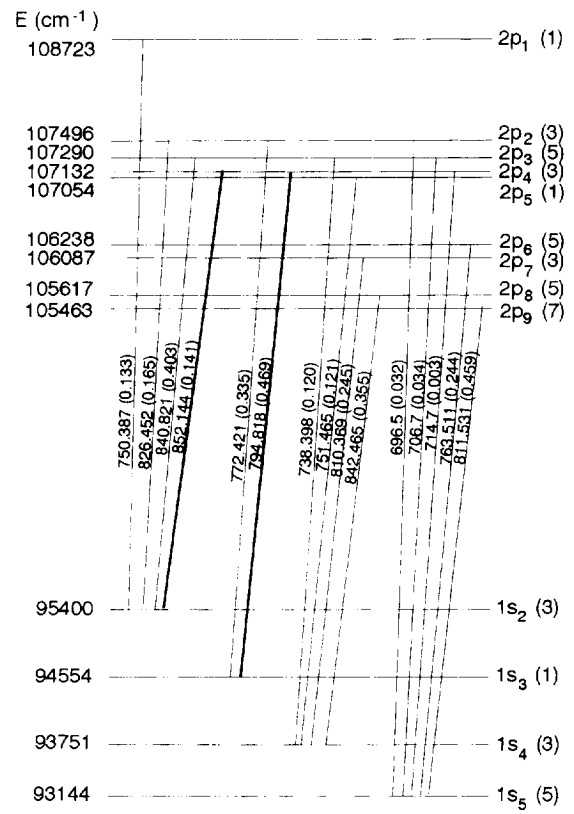

Fig. 1. Part of the energy level scheme of argon atoms, relevant for the experiment, together with the possible transition wavelengths and oscillator strengths. The values between brackets at the right edge of the scheme are the level degeneracies.

degeneracies. To measure the metastable number densities, only the lines starting from the $1s_3$ and $1s_5$ levels can be used. The 794.818 nm line ($1s_3$–$2p_4$) was used for the present experiment, since it has the highest oscillator strength. As a fluorescence line originating from the $2p_4$ level, the 852.144 nm line ($2p_4$–$1s_2$) was measured, because it has the highest oscillator strength. In the present terminology, the $1s_3$ level is called level 1, the $1s_2$ level corresponds to level 2, and the $2p_4$ level is called level 3. From the measured fluorescence intensity, B_F, the population density of level 3, n_3, can be calculated [17]:

$$B_F = h\nu_{32}\left(\frac{\ell}{4\pi}\right)A_{32}n_3$$

where B_F is the fluorescence intensity (in W/cm^2 sr), h is Planck's constant (J s), ν_{32} is the frequency (Hz) corresponding to the fluorescence line, ℓ is the length (cm) in which fluorescence emission can occur (i.e. the laser beam width, i.c. 0.1 cm), A_{32} is the Einstein transition probability of the fluorescence line (1.298×10^7 s^{-1} [16]) and n_3 is the population density of level 3 (cm^{-3}).

From n_3, the population density of level 1 (i.e. $1s_3$ metastable level) can be deduced. In the following, it is shown that the laser pumping rate is much higher than the loss rates. Indeed, the pumping rate is determined by $B_{ij}\rho_\lambda$ (i is level 1 and j is level 3), where the laser spectral energy density ρ_λ (J cm^{-3} cm^{-1}) is given by [17]:

$$\rho_\lambda = \frac{E_L}{s_L \Delta\lambda_{laser} c}$$

where E_L is the laser power (i.c. 170 mW), s_L is the laser spot size (i.c. 7.85×10^{-3} cm^2), $\Delta\lambda_{laser}$ is the line width (FWHM) of the laser excitation ($1s_3$–$2p_4$) line (i.c. ca. 0.0022 nm) and c is the speed of light (cm s^{-1}). Substituting all these values yields: $\rho_\lambda = 3.281$ J cm^{-3} cm^{-1}. The Einstein transition probability B_{ij} (cm^3 cm J^{-1} s^{-1}) is calculated as [17]:

$$B_{ij} = B_{13} = \frac{A_{31} g_3 \lambda^5}{8\pi h g_1 c}$$

where A_{31} is the Einstein spontaneous transition probability of the 3–1 transition (ca. 1.651×10^7 s^{-1} [16]), g_3 and g_1 are the degeneracies of levels 3 and 1 (i.c. 3 and 1, resp.), λ is the wavelength of the 1–3 transition, h is Planck's constant (J s) and c is the speed of light (cm s^{-1}). The factor (λ^2/c) arises as a result of converting $\Delta\nu$ to $\Delta\lambda$ in the definition of ρ_λ above. Substituting all the numerical values yields: $B_{13} = 3.15 \times 10^8$ cm^3 cm J^{-1} s^{-1}. The laser pumping rate then amounts to 1.03×10^9 s^{-1}, which is much higher than the possible radiation loss rates (i.e., the gA values of the fluorescence transitions from level 3 are in the order of 10^7 s^{-1}). Moreover, it was also tested that the laser pumping rate is clearly dominant over the collisional loss rates. Indeed, taking a complete fluorescence spectrum of all lines involving the Ar metastable levels, only the three lines starting from the $2p_4$ level are observed (i.e. the 794.818 nm laser excitation line (resonance fluorescence), the 852.144 nm and the 714.7 nm direct line fluorescence lines). Therefore, collisional mixing of the 2p levels seems to be very low and hence collisional loss rates are negligible compared to the laser pumping rate.

When the laser pumping rate is much higher than the loss rates, the system quickly reaches a steady-state equilibrium in which stimulated emission starts to play a role as the major deexcitation process (saturation). The populations of the excited state and the ground state are then locked with each other and the ratio of these populations is determined only by the level degeneracies. The metastable level population (level 1, $1s_3$) is then calculated from the excited level population (level 3) by [17]:

$$\frac{n_{met(1s_3)}}{n_3} = \frac{g_1}{g_3}$$

Introducing values for the level degeneracies ($g_1 = 1$, $g_3 = 3$) yields: $n_{met(1s_3)} = \frac{n_3}{3}$.

To investigate the role of argon metastable atoms in the glow discharge, the total metastable density (i.e. the sum of the $1s_3$ and $1s_5$ levels) is of interest. It is generally known that the $1s_3$ level is less populated than the $1s_5$ level. According to the level degeneracies, the $1s_5$ level would be five times more populated than the $1s_3$ level. In Ref. [18] it is stated that the concentration of the $1s_3$ level is 10–15% of that of the $1s_5$ level. The level populations of the $1s_3$ and $1s_5$ levels have been measured in Ref. [7] for different pressures and currents, and it was found that the $1s_5$ level is about seven times more populated than the $1s_3$ level. Therefore, the total metastable density is given

by:

$$n_{met} = n_{met(1s_3)} + n_{met(1s_5)} = n_{met(1s_3)} + 7n_{met(1s_3)} = 8n_{met(1s_3)}$$

3. Experimental setup

A Ti:sapphire laser (Schwartz Electro-Optics, Orlando, FL) was used to excite the metastable ($1s_3$) level. It is a passive solid-state laser pumped by the all-lines, continuous-wave output from an argon ion laser (model 2060, Spectra Physics, Mountain View, CA). The Ti:sapphire laser beam has a spectral line width of 10 MHz (based on manufacturer's specifications) and a coherence length of 10 m while operating in the ring configuration. With the currently installed mirror set, the laser is tunable from 780 to 825 nm. Coarse tuning of the laser is done by a birefringent filter, while fine adjustment is accomplished by changing the angle of an intracavity etalon. Because of the narrowness of the laser and atom lines, it was difficult to keep the laser spectrally tuned to the argon line in a stable manner. To overcome this problem, the laser was scanned back and forth over the argon line. In this way, the peak of the signal would reveal the center of the argon absorption transition. To do this, a stepping motor was attached to the tuning micrometer thimble. The motor was manipulated with a controller (model STMC 4, American ISA Inc.) which was set to cycle over the argon line repetitively.

A laser power of 170 mW was used, so that saturation of the excitation line was obtained. The laser beam was focused into the glow discharge chamber by a 25.4 cm focal length fused silica lens. The emitted fluorescence was imaged onto a monochromator (GCA McPherson, model 218) entrance slit by a biconvex fused silica lens. The slit width was 300 μm and the slit height 1 mm, for both the entrance and the exit slit, to provide good spatial resolution. The signal was detected with a PMT (R955, Hamamatsu Corp., Bridgewater, NJ) conditioned with transimpedance amplifier (Model 427, Keithley Instruments, Cleveland, OH), and read out on a strip chart recorder.

The glow discharge chamber was formed by a six-way cross with 4 cm diameter ports made of stainless steel. The four ports in the xy plane were provided with quartz windows. Two of these ports were used for the fluorescence measurements. The other two ports, in the z-direction, were used for the insertion of the cathode probe and as a connection to the vacuum pump, respectively. The entire glow discharge cell was grounded and served as anode, whereas the cathode was at high voltage. Tantalum disks of about 1 mm thick and 4.5 mm in diameter were used as the cathode. These disks were cut from a tantalum rod (99.99% pure, Alfa Aesar, Ward Hill, MA) and glued onto the cathode insertion probe using silver-impregnated paint. A PTFE tube was placed around the tip of the insertion probe so that only the front of the Ta sample was exposed to the discharge plasma. The glow discharge chamber was mounted on a table which could be moved in the x, y and z directions. Three-dimensional spatially resolved profiles were obtained by measuring the fluorescence at every millimeter close to the cathode (up to 6 mm) and at every 2 mm further away from the cathode. Different x–y combinations which corresponded to the same radial distance from the cell axis were found to give the same fluorescence signal. This demonstrated that the discharge could be considered cylindrically symmetrical and that the incoming laser beam and outcoming fluorescence beam were not further absorbed in the glow discharge plasma. Schematic overviews of the experimental setup and of the six-way cross glow discharge are presented in Fig. 2(a) and (b), respectively.

To calculate the metastable population density from the fluorescence radiance, the latter must be expressed in W/cm^2 sr. However, on the chart recorder, the final fluorescence radiance is read out in volts. The conversion from V to W/cm^2 sr is accomplished in the following way. The fluorescence radiance (W/cm^2 sr) is given by the signal output (V), divided by (i) the gain of the electronics (10^6 V/A), (ii) the response of the monochromator and the PMT (in A/W; obtained by calibrating the system, see below), (iii) the monochromator entrance slit area corrected for magnification due to the optics (300 μm × 1 mm / 1.35 = 0.0022 cm^2), (iv) the solid angle of the optical system (0.0276 sr), and (v) the transmission of the window of the glow discharge chamber (measured as 0.8317) and the optical lens between the glow discharge chamber and monochromator (0.92 on the assumption of 4% surface losses at each side). In the calculation of the solid angle of the optical

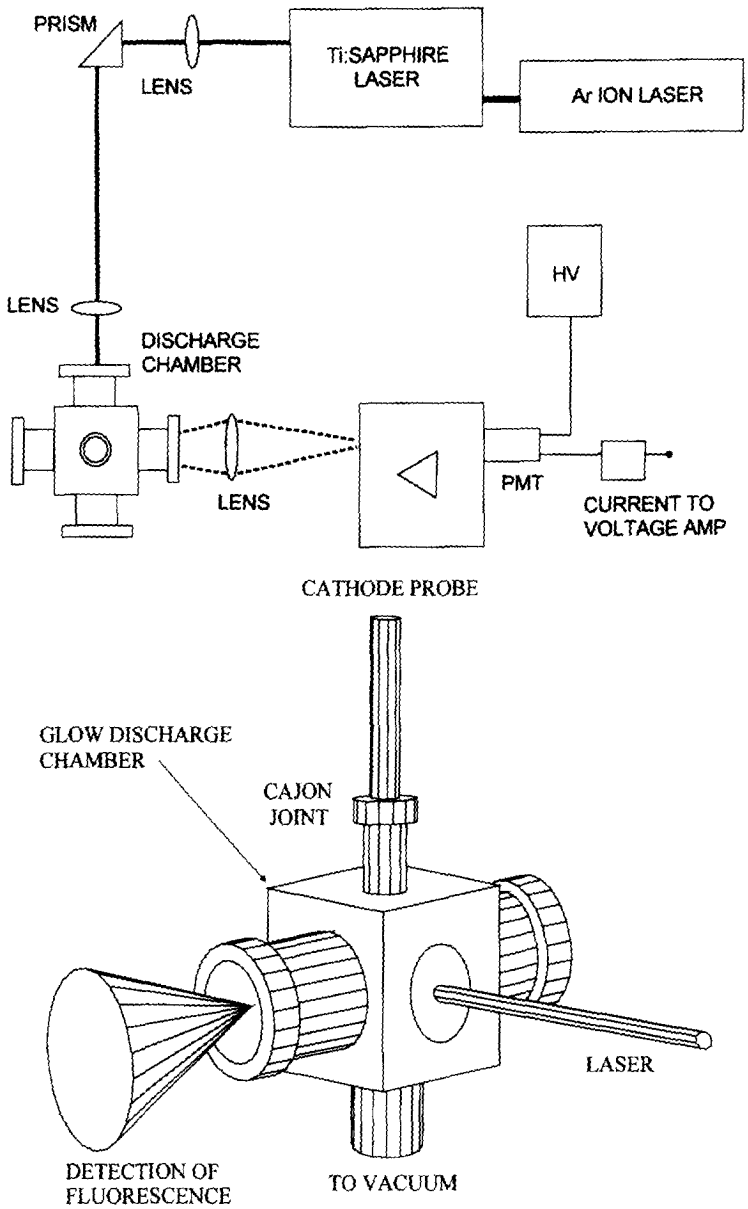

Fig. 2. Schematic overview of the experimental setup (a) and the glow discharge six-way cross geometry (b).

system, any chromatic aberrations were assumed to be absent.

The calibration of the monochromator and PMT was carried out by scattering about 3 mW of laser radiation at 825 nm from a frosted fused silica plate placed at 45° on the central axis of the glow discharge chamber. The scattered radiation was imaged upon the entrance slit of the monochromator via the identical optical system used for the fluorescence measurements. A calibrated photodiode (United Detector Technologies, PIN–10DP) was placed behind the entrance slit of the spectrometer, where 45.9 nW was detected. This amount of radiation produced a photocurrent of 135 μA on the photomultiplier. Therefore, the response of the monochromator and PMT is 2941 A/W at 825 nm. Relative calibration to

the fluorescence wavelength (852 nm) was carried out by using a 1000 W quartz–halogen tungsten coiled-coil filament lamp (model FEL–C) and yielded a value of 531.1 A/W for the response of the monochromator and PMT at 852 nm and a PMT voltage of 1000 V.

4. Mathematical model

A mathematical model for the argon metastable atoms has been developed in one dimension [9] and in three dimensions for the standard cell for analysing flat samples in the VG 9000 glow discharge mass spectrometer [10]. The model is based on a balance equation with all known production and loss processes. The production processes include electron, argon ion and atom impact excitation, and argon ion–electron radiative recombination. The loss processes comprise electron impact ionization and excitation from the metastable level, transition to the nearby resonant levels due to collisional quenching by slow electrons, metastable–metastable collisions, Penning ionization of sputtered atoms, two-body and three-body collisions with argon ground state atoms, and diffusion and subsequent de-excitation at the walls. A detailed description of this model is found in Refs. [9,10]. The three-dimensional model of Ref. [10] was modified and applied to a cylindrical cell geometry approximating the experimental six-way cross geometry (i.e. 4 cm diameter, 2 cm length and a Ta cathode of 4.5 mm diameter), in order to be able to compare experimental and modeling results.

The metastable density calculated in the model depends on the assumptions made about the various production and loss processes. For the discharge conditions used in the experiment (1000 V, 1 torr, 2 mA), it was found that the dominant production processes are electron, argon ion and atom impact excitation to the metastable levels. Electron impact excitation is especially important in the beginning and center of the negative glow (i.e. about 3–6 mm from the cathode) where the electrons have the most suitable energies for this process (about 20–100 eV). Argon ion and atom impact excitation are only significant close to the cathode where the argon ions and atoms reach high energies (i.e. about 30–100 eV on average). Since the cross-sections of these three processes are of comparable magnitude [19,20] and since the argon ion and atom fluxes are higher than the electron flux [21,22], the excitation rates by ion and atom impact (calculated in the present case to be about $4 \times 10^{16}\,cm^{-3}\,s^{-1}$ and $10^{17}\,cm^{-3}\,s^{-1}$ at the maximum, respectively) are higher than the excitation rate by electron impact (calculated to be about $10^{16}\,cm^{-3}\,s^{-1}$ at the maximum). Since the ion and atom impact excitation is more or less concentrated in the first millimeter from the cathode whereas electron impact excitation is spread out over a wider region, the relative contributions of ion, atom and electron impact excitation to the production of argon metastable atoms amount to about 12%, 43% and 45%, respectively, integrated over the total discharge volume. Loss of the argon metastable atoms is, according to the calculations, primarily due to diffusion and subsequent de-excitation at the walls (especially dominant close to the cathode, spreading out the high production by ion and atom impact excitation), and transition to the nearby $1s_2$ and $1s_4$ levels by collisional quenching with slow electrons (particularly important in the negative glow where slow electrons are present). Integrated over the complete three-dimensional volume, it was calculated that diffusion and electron quenching each contribute to about 45.5% and 49%, respectively, whereas the remaining losses are due to metastable–metastable collisions (ca. 3%), Penning ionization of sputtered Ta atoms (ca. 1.5%) and electron impact excitation (ca. 1%) from the metastable levels. Electron impact ionization from the metastable levels and two-body and three-body collisions were found to be negligible under the present discharge conditions.

5. Results and discussion

Fig. 3 shows a three-dimensional number density profile of the argon metastable atoms, measured at 1000 V, 1 torr and 1.8 mA. Since the glow discharge plasma extends in nearly a cylindrical way, the three-dimensional profile can be presented as a two-dimensional cross-section of the cell. The cathode of the cell is illustrated with the black line at $r = 0$ and $z = 0$ on the figure. The argon metastable density reaches a maximum at a few millimeters from the cathode in the axial direction, drops to a local minimum at about 7 mm and increases

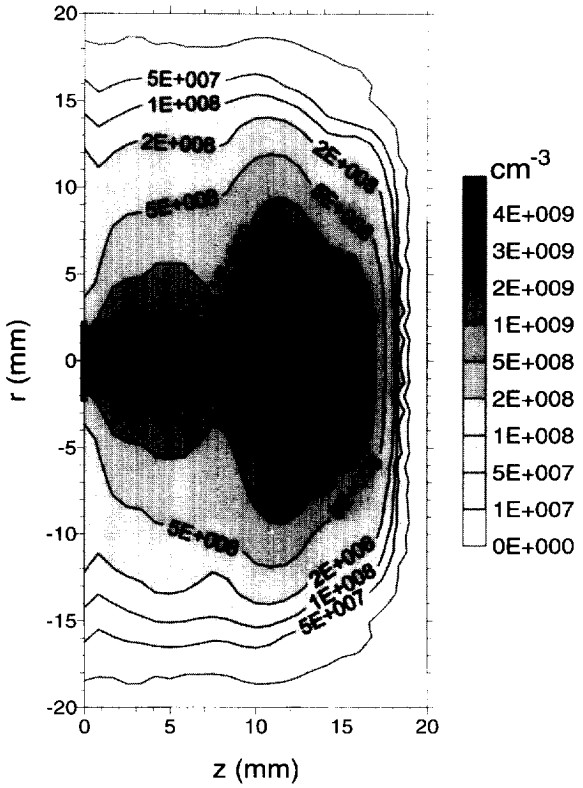

Fig. 3. Argon metastable density profile measured by laser-induced fluorescence, at 1000 V, 1 torr, 1.8 mA.

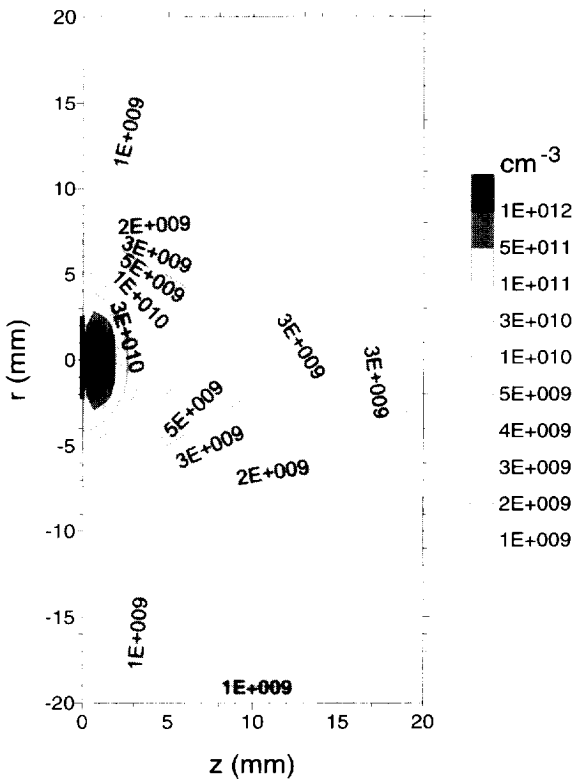

Fig. 4. Argon metastable density profile, calculated by the model, at 1000 V, 1 torr, 2 mA.

again to a second maximum at about 12 mm from the cathode. In the radial direction it decreases gradually towards the cell walls. The measurements were performed for a range of different voltages and pressures, and the occurrence of two maxima (the first at 2–4 mm and a second one, slightly lower, at about 12 mm) is always observed. In some cases, there was also a maximum at about 16 mm, or two distinct maxima at 2–4 mm, as in Fig. 3. It is not clear whether the two maxima at 2 and 4 mm are real or just artefacts, because there is only one measuring point between them, at 3 mm. However, the occurrence of at least one maximum at 2–4 mm and another one at about 12 mm was very reproducible throughout all the measurements and is therefore assumed to be real.

At first sight, this profile looks rather unexpected. However, when we compare it with the theoretically calculated argon metastable density profile presented in Fig. 4, we see that the modeling result also shows such a profile. It is not completely the same, i.e. the calculated profile shows a pronounced maximum at about 1 mm from the cathode and a second lower maximum at about 18 mm from the cathode.

The occurrence of these maxima can be adequately explained by the different production and loss processes in the model (see Section 4). Indeed, the first maximum in front of the cathode is caused by argon ion and atom impact excitation. Electron impact excitation would be responsible for a second maximum in the beginning of the negative glow, but this production is almost entirely compensated by the loss due to electron quenching. At the end of the negative glow, the number density of slow electrons has dropped so much that electron quenching becomes negligible and a net production by electron impact excitation is observed, giving rise to the second peak at about 18 mm. Since the net production processes are rather localized, the diffusion process is not able to spread out the production of metastables completely from one maximum to the other; therefore distinct maxima

remain in the metastable density profile. The occurrence of two distinct maxima in the argon metastable atom density profile was also observed for a Grimm-type glow discharge in Ref. [14].

The fact that the modeling result (Fig. 4) is not completely similar to the experimental result (Fig. 3) indicates that the production and loss processes incorporated in the model do not yet completely describe the real situation. It can be understood that it is indeed difficult to reach complete agreement, due to the complexity and diversity of the different production and loss processes and the rather large uncertainties in the rate constants of some of these processes. It is possible that the two peaks present in the experimental profile are caused by the same production and loss processes as the two peaks in the calculated profile, i.e. that the location of the various production and loss processes is not yet correctly described in the model. Because of the uncertainties in the rate constants, the magnitude and hence the relative importance of the different production and loss processes may not yet be correctly described in the model, leading to a local maximum at the wrong position.

On the other hand, it may also be that the present model is not yet complete and that other production and/or loss processes have to be included in order to reach agreement with experiment. In particular, the high peak close to the cathode in the calculated result is in disagreement with the measured profile. Indeed, comparison of the numerical values in Figs 3 and 4 shows that the experimental and theoretical results are in reasonable agreement with each other, except in the first few millimeters where the calculated density is almost two orders of magnitude higher than the experimentally obtained values. This would indicate that either the production process by ion and atom impact excitation is overestimated or that additional loss processes occur in this region which are not incorporated in the model. In Ref. [20], it is indeed suggested that the cross-sections of argon ion and atom impact excitation to the metastable levels have to be considered as upper limits. We had somewhat arbitrarily lowered them already by a factor of 2, so that the maximum in these cross-sections became equal to the maximum in the cross-section for electron impact excitation to the metastable level. This is based on the assumption that the mechanisms of these processes are similar, so that their cross-sections are also

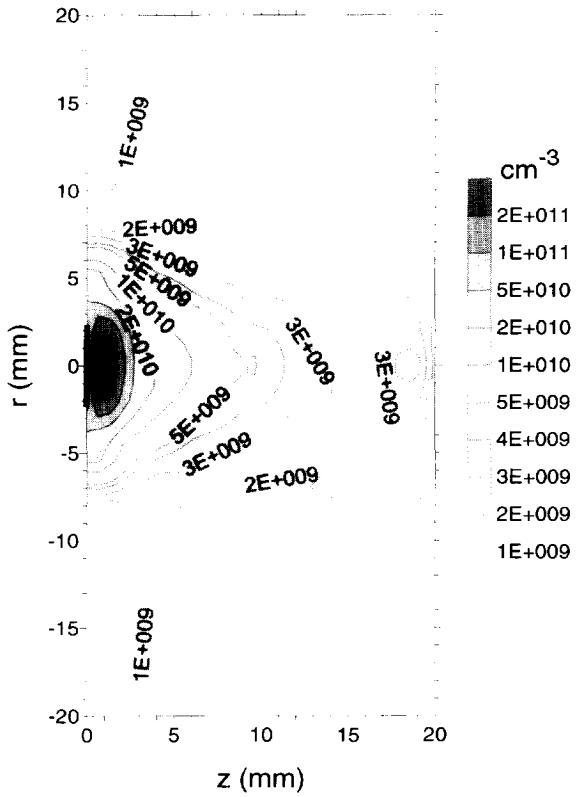

Fig. 5. Calculated argon metastable density profile at 1000 V, 1 torr, 2 mA, obtained by lowering the cross-sections of argon ion and atom impact excitation to the argon metastable levels by a factor of 10.

of equal magnitude. Because the calculated peak is almost two orders of magnitude too high, the cross-sections of these processes were further lowered by factors of 10 and 100; these results are presented in Figs 5 and 6, respectively. Lowering the cross-sections by a certain factor does not, however, yield a linear decrease in the peak maximum since the loss by diffusion also decreases. Hence, dividing the cross-sections by a factor of 10 resulted in a decrease in the peak value by a factor of only 5 (see Fig. 5), and lowering them by a factor of 100 resulted in a drop in peak intensity of only 10 (see Fig. 6). The number density profile at distances further away from this peak remains unchanged. Even when the cross-sections are lowered by a factor of 100, which seems rather unrealistic, the peak is still too high.

This suggests that there must be an additional loss

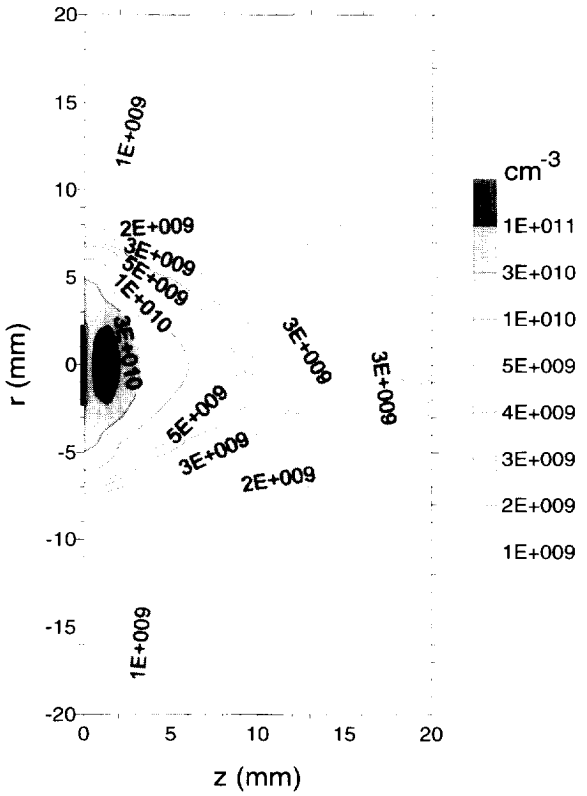

Fig. 6. Calculated argon metastable density profile at 1000 V, 1 torr, 2 mA, obtained by lowering the cross-sections of argon ion and atom impact excitation to the argon metastable levels by a factor of 100.

process close to the cathode, to compensate for the high production of metastable argon atoms by ion and atom impact excitation. A possible candidate would be argon ion and atom impact ionization and excitation from the metastable level, in analogy to electron impact ionization and excitation from the metastable level. These processes may seem quite exotic, but it can be expected that they occur, since ion and atom impact ionization and excitation from the ground state also play a significant role close to the cathode. However, the cross-sections of these processes are not available in the literature. A rapid calculation, based on cross-section values similar to those for electron impact ionization and excitation, shows that these processes are still a factor of 30 less important than argon ion and atom impact excitation from the ground state to the metastable level, since the metastable densities are still four orders of magnitude lower than the ground state density.

Another possibility is some process like electron collisional transition to the nearby $1s_2$ and $1s_4$ levels in the negative glow, since this process has a high rate constant. However, such a process is not known in the literature, and this assumption can therefore not be checked.

In any case, it was found that the peak in the metastable number density close to the cathode does not have so much influence on the overall picture of the glow discharge. Indeed, the argon metastable atoms are of particular interest in the glow discharge for their role in the ionization of sputtered atoms (Penning ionization). In the model, the number density of tantalum (sputtered species) ions is calculated as a result of electron impact ionization, Penning ionization by argon metastables and asymmetric charge transfer by argon ions [10,23]. When the cross-section of ion and atom impact excitation to the argon metastable levels was lowered by a factor of 100, the density of the tantalum ions at the maximum of its profile changed only from $9.511 \times 10^9\,cm^{-3}$ to $9.504 \times 10^9\,cm^{-3}$, since the metastable density in the rest of the discharge remained unchanged and since asymmetric charge transfer was found to be more important than Penning ionization [24]. Hence, although the model cannot yet predict the exact metastable number density profile, this discrepancy does not seem to have much effect on the overall 'analytical' picture of the discharge.

To test the effect of voltage, pressure and current on the metastable density profile, fluorescence measurements were performed for a range of different discharge conditions. The influence of voltage and current on the one-dimensional density profile on the cell axis at constant pressure is presented in Fig. 7(a), and the effect of pressure and current at constant voltage is illustrated in Fig. 7(b). It is seen that the metastable number density generally increases with voltage, pressure and current. The curves are not very smooth, but it is clear that at least two peaks can be distinguished in all cases. The first peak at 2–4 mm is always the most intense one, but at high voltages, pressures and currents the second one at about 12 mm is gaining importance and even a third peak seems to appear at about 17 mm.

The metastable densities are found to be in the order of $5 \times 10^9\,cm^{-3}$ to $6 \times 10^{10}\,cm^{-3}$ over the

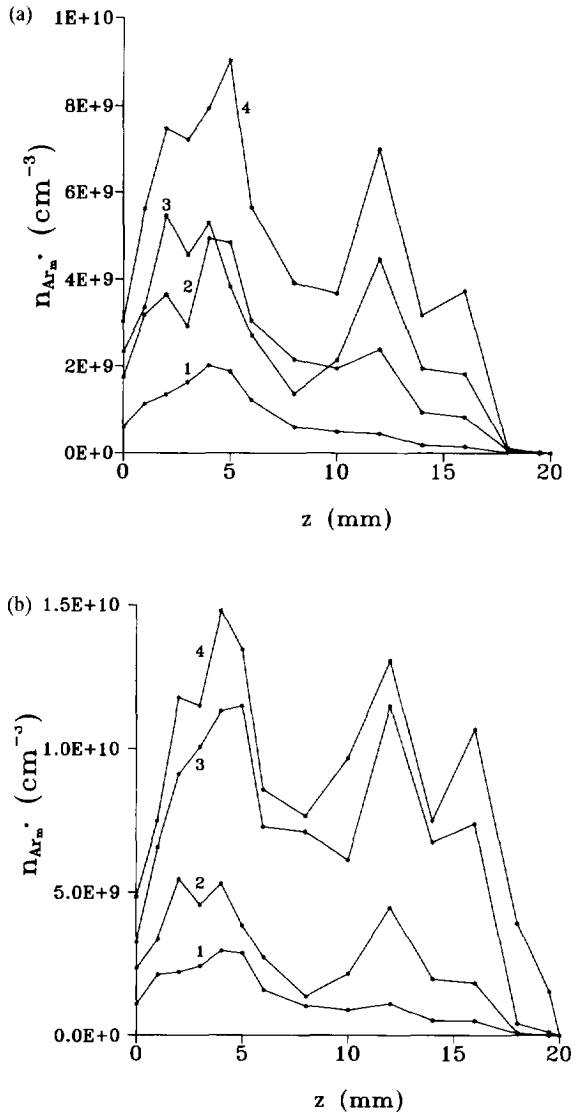

Fig. 7. One-dimensional argon metastable density profiles at the cell axis, measured by laser-induced fluorescence: (a) at 1 torr and different voltages (1: 700 V, 0.6 mA; 2: 850 V, 1.3 mA; 3: 1000 V, 1.8 mA, 4: 1200 V, 2.3 mA), and (b) at 1000 V and different pressures (1: 0.7 torr, 0.8 mA; 2: 1.0 torr, 1.8 mA; 3: 1.3 torr, 2.45 mA; 4: 1.6 torr, 3.3 mA).

range of the discharge conditions. This is somewhat lower than is often suggested in general overviews on glow discharges. The metastable argon atom density seems therefore to be clearly lower than the argon ion density, which is calculated to be in the order of 10^{11}–10^{12} cm^{-3} for electrical currents of a few mA [22,25]. It is therefore suggested that, for elements which possess suitable energy levels, asymmetric charge transfer could be more important than Penning ionization. For the present discharge conditions, this is indeed calculated to be the case [27].

The metastable densities obtained in this experiment are on the lower side of the values found in the literature (see Introduction). It is very difficult to compare argon metastable densities with densities of helium or neon metastables, since other production and loss processes can be responsible in the case of these species of gases. So it makes sense only to compare them with other argon metastable densities. In Refs. [13,14] argon metastable densities of the order of 10^{11}–5×10^{11} cm^{-3} and 3×10^{12}–10^{13} cm^{-3}, respectively, have been obtained. However, both experiments were performed in a Grimm-type glow discharge, operating at much higher pressures and currents, so that exact comparison is not possible. In Refs. [7,15], metastable argon number densities have been measured in a discharge tube operating at pressures and currents comparable to our conditions. The values obtained are in the order of 2×10^{10}–2×10^{11} cm^{-3}, which is in better agreement with our results. It seems that the metastable number densities can vary over many orders of magnitude for different discharge conditions and geometries. Indeed, when the same model as is presented here is applied to the geometry of the standard cell of the VG 9000 mass spectrometer, which is about half as large, the metastable number densities obtained are generally one order of magnitude higher throughout the discharge cell [10]. When we take into account that such large variations can occur, the present agreement between experiment and theory is very satisfying.

6. Conclusion

Three-dimensional absolute number density profiles of the argon metastable atoms in a direct current glow discharge have been measured with laser-induced fluorescence. The number density profile is characterized by at least two peaks, appearing at 2–4 mm and about 12 mm. This can be explained by the occurrence of local production and loss processes which lead to local maxima that cannot

completely be spread out by diffusion. Such peaks are indeed also observed in the results of a model based on a balance equation with different production and loss processes. The exact position of the peaks and also the absolute value of the first peak are not yet in complete agreement between experiment and theory. This indicates that the glow discharge cannot yet be perfectly described by the model, and that the situation is possibly still more complicated than is often assumed. However, comparing the absolute values of the metastable density further away than a few millimeters from the cathode, it can be concluded that satisfactory agreement is already reached between experimental and theoretical results.

Acknowledgements

A. Bogaerts wishes to thank the Belgian National Fund for Scientific Research (NFWO) for financial support and for the travel grant to the University of Florida. A. Bogaerts and R. Gijbels also acknowledge financial support from the Federal Services for Scientific, Technical and Cultural Affairs (DWTC/SSTC) of the Prime Minister's Office through IUAP-III (Conv. 49). This research has been partially supported by DOE-DE-FG05-88ER13881 and DOE-DE-FG05-89ER114018.

References

[1] W.W. Harrison, Glow discharge mass spectrometry, in F. Adams, R. Gijbels and R. Van Grieken (Eds.), Inorganic Mass Spectrometry, Wiley, New York, 1988, Chap. 3.
[2] R.K. Marcus, Glow Discharge Spectroscopies, Plenum Press, New York, 1993.
[3] E.A. Den Hartog, D.A. Doughty and J.E. Lawler, Phys. Rev. A 38 (1988) 2471.
[4] E.A. Den Hartog, T.R. O'Brian and J.E. Lawler, Phys. Rev. Lett., 62 (1989) 1500.
[5] T. Kubota, Y. Morisaki, A. Ohsawa and M. Ohuchi, J. Phys. D, 25 (1992) 613.
[6] K.A. Hardy and J.W. Sheldon, J. Appl. Phys., 53 (1982) 5832.
[7] C.M. Ferreira, J. Loureiro and A. Ricard, J. Appl. Phys., 57 (1985) 82.
[8] D.P. Lymberopoulos and D.J. Economou, J. Appl. Phys., 73 (1993) 3668.
[9] A. Bogaerts and R. Gijbels, Phys. Rev. A, 52 (1995) 3743.
[10] A. Bogaerts and R. Gijbels, Anal. Chem., 68 (1996) 2676.
[11] P.G. Browne and M.H. Dunn, J. Phys. B, 6 (1973) 1103.
[12] E.W. Eckstein, J.W. Coburn and E. Kay, Int. J. Mass Spectrom. Ion Phys., 17 (1975) 129.
[13] N.I. Uzelac and F. Leis, Spectrochim. Acta B, 47 (1992) 877.
[14] N.P. Ferreira, J.A. Strauss and H.G.C. Human, Spectrochim. Acta B, 37 (1982) 273.
[15] C.M. Ferreira and A. Ricard, J. Appl. Phys., 54 (1983) 2261.
[16] R.S.F. Chang and D.W. Setser, J. Chem. Phys., 69 (1978) 3885.
[17] N. Omenetto and J.D. Winefordner, Prog. Anal. At. Spectrosc., 2 (1979) 1.
[18] J.H. Kolts and D.W. Setser, J. Chem. Phys., 68 (1978) 4848.
[19] N.J. Mason and W.R. Newell, J. Phys. B, 20 (1987) 1357.
[20] A.V. Phelps, J. Phys. Chem. Ref. Data, 20 (1991) 557.
[21] A. Bogaerts, M. van Straaten and R. Gijbels, Spectrochim. Acta B, 50 (1995) 179.
[22] A. Bogaerts, R. Gijbels and W.J. Goedheer, J. Appl. Phys., 78 (1995) 2233.
[23] A. Bogaerts and R. Gijbels, J. Appl. Phys., 79 (1996) 1279.
[24] A. Bogaerts, E. Wagner, B.W. Smith, J.D. Winefordner, D. Pollmann, W.W. Harrison and R. Gijbels, Spectrochim. Acta B, 52 (1997) 205.
[25] A. Bogaerts, R. Gijbels and W.J. Goedheer, Anal. Chem., 68 (1996) 2296.